An automatic algorithm for equivalent circuit extraction from noisy frequency responses

An automatic algorithm for equivalent circuit extraction from noisy frequency responses

S. Grivet-Talocia, M. Bandinu, F. G. Canavero
Dipartimento di Elettronica, Politecnico di Torino,
Corso Duca degli Abruzzi 24, 10129, Torino, Italy
Email: stefano.grivet@polito.it

***Abstract*— This paper presents a fully automatic algorithm for the extraction of equivalent circuits from noisy frequency responses. The application area involves the generation of SPICE-ready macromodels for critical interconnects for Signal Integrity chatacterizations. Direct measurements are often employed to obtain a characterization of a given interconnect structure, leading to its frequency-dependent scattering responses. The proposed technique processes these responses and outputs an equivalent circuit. The algorithm is based on a modification of the well-known Vector Fitting scheme, which has now become a standard tool in EMC and SI studies. The presented improvements focus on robustness to noise, which is always present in measured data, and on automatic order estimation. These issues are addressed via an automatic detection of any spurious poles due to the noise, which are hard relocated in order to maximize the model accuracy. Several application examples are presented to illustrate the excellent capabilities of the new fitting scheme.**

I. Introduction

Electrical interconnects are often responsible for the most relevant deviation of an electronic system from its ideal and desired behavior. This is due to several non-ideal effects like crosstalk, spurious couplings, dispersion, losses, radiation, reflections, and other issues that can be found at various integration levels, from chip to package, from board to system and even interconnected systems. A thorough EMC and SI assessment of a complete system is a very challenging task due to the extreme complexity of state-of-the art high-speed applications.

A common approach to handle these difficulties is to view the entire system as a collection of separate and well-defined multiports such, e.g., segments of dispersive transmission lines interspersed by discontinuities like vias, connectors, and transitions. Each of these structures can be characterized separately via direct measurement (if possible) or electromagnetic simulation to obtain its frequency-domain port responses, usually scattering parameters. These responses are in turn fed to fitting algorithms that produce rational approximations of the scattering matrix in the Laplace domain. Synthesis of lumped circuit equivalents from these rational approximations is straightforward. As a result, this strategy allows to carry out a detailed system-level analysis, including signal degradation effects, using commonly available circuit solvers such, e.g., SPICE.

Several fitting algorithms are available for the rational approximation generation. Among these, the Vector Fitting (VF) algorithm [1] has become very popular in the last few years, and many successful applications have already been documented [2]. The main reason for this success is the smart formulation of the rational approximation process, which is cast in terms of an iterative sequence of steps, each corresponding to the solution of a simple and well-conditioned linear system [3]. This formulation provides much better numerical stability and robustness with respect to more classical rational approximation schemes.

This study addresses the behavior of VF algorithm in presence of noise in the original frequency responses that characterize the structure under investigation. This issue is relevant every time the responses come from direct VNA measurement. The extensive tests that we performed show that noise can significantly impair convergence, leading to possibly inaccurate models due to the presence of noise-induced spurious poles. We document these difficulties in Section III, and we present a possible solution in Section IV. We show that a simple test allows to detect the spurious poles. We also introduce an incremental pole addition scheme that, combined with the removal of spurious poles, leads to a robust algorithm with automatic order estimation capabilites. Several numerical tests and applications, presented in Section V, illustrate and validate the algorithm.

II. Background: the Vector Fitting algorithm

Let us consider a structure characterized by its transfer function $H(s)$, to be approximated by a rational expression

$$H(s) \simeq H_\infty + \sum_{n=1}^{N} \frac{r_n}{s - p_n} \tag{1}$$

with unknown poles $\{p_n\}$ and residues $\{r_n\}$. The approximation (1) is to be computed starting from a set of frequency samples $H(j\omega_k)$. Standard VF is an iterative algorithm that refines an initial estimate $\{q_n^0\}$ of the N dominant poles of the structure. The set of poles that is obtained at the i-th iteration is denoted as $\{q_n^i\}$. The weight function

$$\sigma^i(s) = 1 + \sum_{n=1}^{N} \frac{k_n^i}{s - q_n^i} = \frac{\prod_{n=1}^{N}(s - z_n^i)}{\prod_{n=1}^{N}(s - q_n^i)} \tag{2}$$

with unknown residues $\{k_n^i\}$ is employed to enforce the following condition

$$\sigma^i(s)H(s) \simeq c_\infty^i + \sum_{n=1}^{N} \frac{c_n^i}{s - q_n^i}, \qquad s = j\omega_k \tag{3}$$

0-7803-9380-5/05/$20.00 ©2005 IEEE.

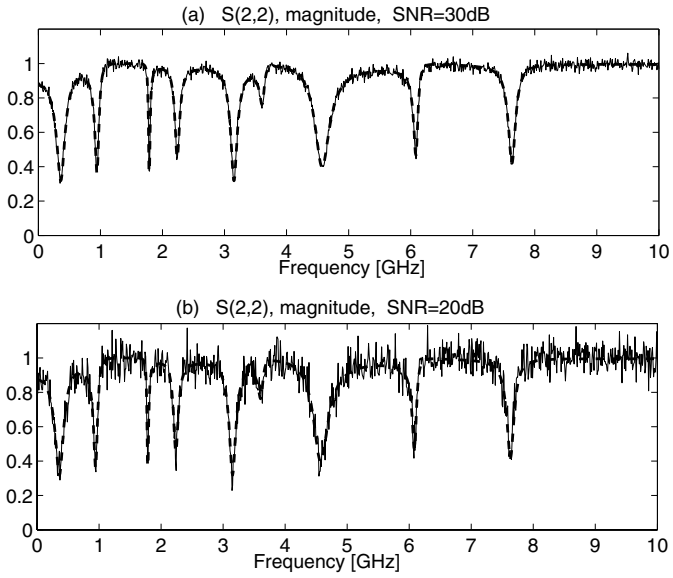

Fig. 1. Two realizations of noisy scattering responses. The magnitude of S_{22} is reported for SNR=30 dB (a) and SNR=20 dB (b). Thin lines represent the noisy responses, whereas thick dashed lines indicate the clean responses before noise addition.

in least-squares sense, using the available data $H(j\omega_k)$. The solution of the linear system (3) provides the residues $\{k_n^i\}$ of $\sigma^i(s)$, which are used to compute the zeros $\{z_n^i\}$ by solving a simple eigenvalue problem [1]. It can be shown that these zeros provide an improved estimate for the poles, that can be used for next iteration, i.e.,

$$q_n^{i+1} = z_n^i\,, \qquad n = 1, \ldots, N \tag{4}$$

Iterations are stopped when the desired accuracy is reached. In absence of noise, usually very few iterations (from one to three-four) are necessary. Once the poles are known, a second linear least-squares solution to Eq. (1) provides the residues $\{r_n\}$. A full description of the VF scheme with extensions to the matrix case can be found in [1], [3].

III. Effects of noise

To investigate the sensitivity of the VF scheme to noise, we devised a process for the generation of synthetic rational scattering matrices characterized by prescribed number of poles N and ports P. The (stable) poles can be placed arbitrarily in a region $[-\vartheta B, 0] \times [-B, B]$ of the complex plane, where B is the bandwidth and ϑ is a parameter allowing to control the amount of losses. The synthesis scheme is documented in [4], where we show that also passivity is guaranteed, so that the synthetic responses are very similar to the responses of real interconnect structures. This process leads to randomly-generated rational scattering matrices of the form

$$\boldsymbol{S}(s) = \boldsymbol{S}_\infty + \sum_{n=1}^{N} \frac{\boldsymbol{R}_n}{s - p_n}\,. \tag{5}$$

Noisy responses are then generated from (5) as

$$\widehat{S}_{ij}(j\omega_k) = S_{ij}(j\omega_k) + N_{ij}(\omega_k)\,, \tag{6}$$

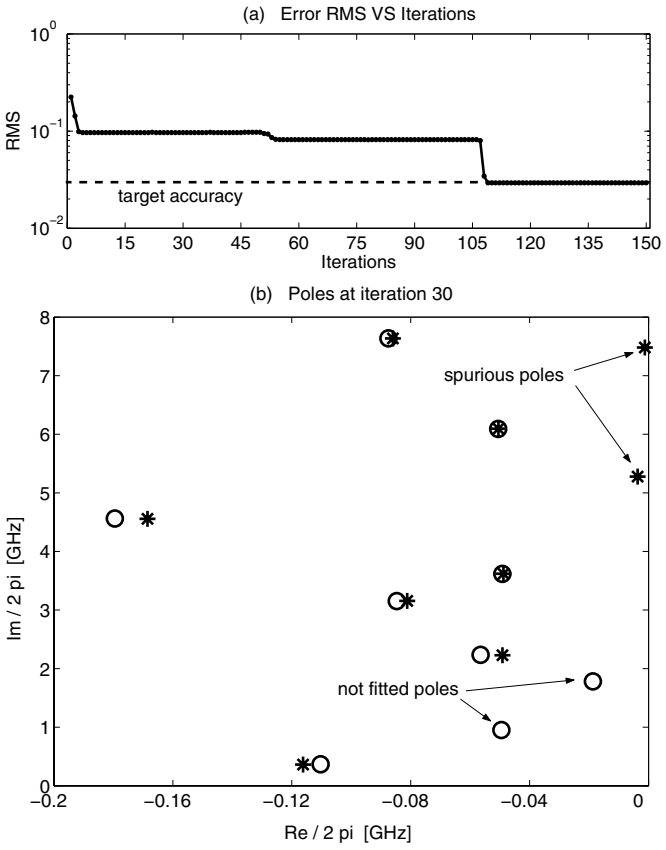

Fig. 2. (a) evolution of the approximation error $\widehat{\varepsilon}$ during the VF iterations applied to a noisy response with SNR=30 dB; (b) spurious poles affecting the convergence (circles: true poles, stars: macromodel poles).

where $N_{ij}(\omega_k)$ represents a sequence of statistically independent and complex-valued random variables. Both real and imaginary parts are assumed to have a zero-mean Gaussian distribution with a variance which is parameterized by the Signal to Noise Ratio (SNR), defined as

$$\mathrm{SNR}_{\mathrm{dB}} = 10 \log_{10} \frac{||S_{ij}||^2}{||N_{ij}||^2}\,, \tag{7}$$

and where the RMS norm is used. In all numerical experiments we performed, the SNR is kept constant for all transfer matrix entries, in order to simplify the statistical analysis of the results. Examples of noisy responses ($N = 18$, $P = 1$, $\vartheta = 0.01$) with a SNR of 20 dB and 30 dB, respectively, are shown in Fig. 1.

Basic VF algorithm was applied to recover estimates of the N poles and residues matrices in (5) starting from these noisy frequency responses. Denoting the transfer matrices of the macromodels as $\boldsymbol{S}^{\mathrm{fit}}(j\omega)$, the corresponding approximation error can be defined as

$$\widehat{\varepsilon} = ||\boldsymbol{S}^{\mathrm{fit}}(j\omega) - \widehat{\boldsymbol{S}}(j\omega)|| = \max_{i,j} ||\Delta_{ij}(\omega)||\,, \tag{8}$$

where

$$\Delta_{ij}(\omega) = |S_{ij}^{\mathrm{fit}}(j\omega) - \widehat{S}_{ij}(j\omega)| \tag{9}$$

represents the frequency-dependent model deviation for the (i,j) matrix entry, and where the RMS (energy) norm is used. Since the "raw" dataset $\widehat{\boldsymbol{S}}(j\omega)$ is affected by noise, it is not possible to achieve convergence down to arbitrary precision, since the noise variance determines an upper bound on the achievable accuracy of the fit. More precisely,

$$\min\{\widehat{\varepsilon}\} \simeq ||\boldsymbol{N}(j\omega)|| = \widehat{\varepsilon}_{\rm opt}\,, \tag{10}$$

where the minimum is taken among all possible macromodels (with the same number of poles N). We denote the quantity $\widehat{\varepsilon}_{\rm opt}$ as *target accuracy*.

The results for a representative case are shown in Fig. 2. The error decay during the VF iterations is depicted in panel (a). These results indicate that VF stagnates in some kind of local minimum during the search of the optimal fit through the iterations. Moreover, the decrease in the fitting error occurs abruptly, with a possibly large number of iterations required before a significant accuracy improvement is observed. It turns out that the reason for this error stagnation is the presence of spurious poles, depicted at iteration 30 in Fig. 2b. These poles are locked through the iterations since they try to fit the noise instead of the true data. Equivalently, it can be stated that the VF condition (3), which is the only constraint leading to poles relocation in the basic VF algorithm, is not strong enough to force the spurious poles to converge to their expected location. A significant improvement of the fitting scheme would be expected if the spurious poles could be automatically detected and relocated closer to the true ones. These two issues are addressed next.

IV. A ROBUST FITTING ALGORITHM

We consider first the detection of the spurious poles. We define a pole to be spurious if its contribution to the rational approximation is negligible. After extensive testing we selected the following criterion based on the energy of the associated resonance curve. Given a single pair of complex conjugate poles $\{p_n, p_n^*\}$ and residues $\{r_n, r_n^*\}$ of the macromodel, we define a bandlimited norm as

$$\mu_n = \left(\int_{\Omega_n} \left| \frac{r_n}{j\omega - p_n} + \frac{r_n^*}{j\omega - p_n^*} \right|^2 d\omega \right)^{1/2} \tag{11}$$

where the integral is over the -10dB bandwidth Ω_n. Note that this bandwidth is always limited by an upper frequency since $|H_n(j\omega)|$ decays as -20dB per decade at high frequencies. A pole pair is considered to be spurious when

$$\frac{\mu_n}{\langle \mu \rangle} < \gamma \ll 1 \tag{12}$$

where $\langle \mu \rangle$ represents the average among the norms associated to all poles, and γ is a suitable threshold that controls how sensitive should be the detection. Typical convenient values range from $\gamma = 0.01$ to $\gamma = 0.05$. The extension of the detection process to real poles is obvious.

When some spurious poles are found, there are two possibilities. One is simply to remove them. However, this would reduce the total number of poles of the rational approximation, leading to no accuracy improvements. We prefer to use a hard relocation strategy that removes the spurious poles and adds new poles in locations of the complex plane that are likely to be close to the true dominant poles of the structure. If the number of poles that is inserted equals the number of detected spurious poles, the order of the macromodel is kept constant. If instead the number of the added poles is larger, the order increases through the iterations. Using an appropriate stopping condition based on the accuracy, it is therefore possible to estimate the optimal number of poles that guarantee a good fit within a prescribed error tolerance.

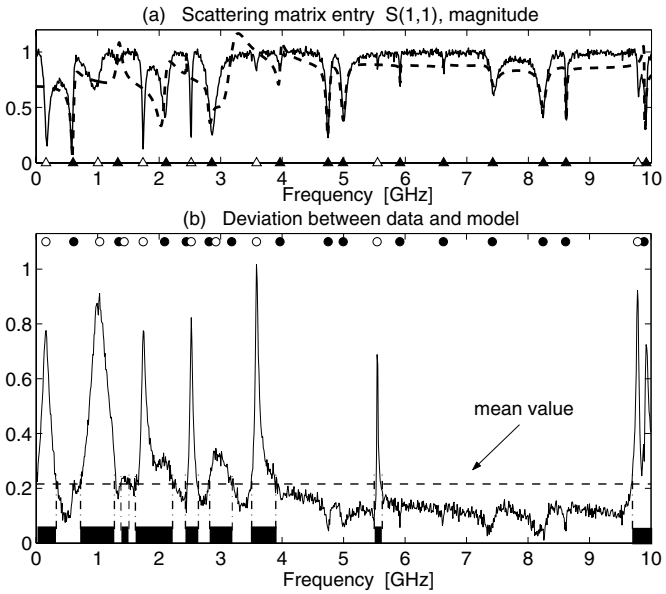

Fig. 3. Characterization of the pole addition process (see text).

We consider the general situation depicted in the top panel of Fig. 3. The plot reports a noisy response $\widehat{S}_{11}(j\omega)$ of a synthetic two-port rational scattering matrix having 40 poles, with a superimposed Gaussian noise with a Signal to Noise Ratio (SNR) of 30 dB. The dashed line is the response of a model having only $N = 30$ poles, obtained via standard VF after 4 iterations. The difference between model and data is evident, mainly due to the insufficient number of model poles. This number is not known a priori. The frequencies of all poles of the original transfer matrix are denoted by triangles in the top panel, with filled triangles indicating those poles that have been reasonably approximated in the model, and empty triangles indicating the poles that still need to be identified and approximated. In order to increase the set of model poles, we consider the frequency-dependent error $\Delta_{ij}(\omega)$ between model and data, reported in the bottom panel of Fig. 3. We define a set of separate bandwidths Ψ_{ij}^n where $\Delta_{ij}(\omega)$ exceeds its mean value. These bands are highlighted by thick segments in the plot. For each Ψ_{ij}^n, we search the local maximum M_{ij}^n of $\Delta_{ij}(\omega)$. The corresponding frequencies $\omega_{\rm max}^n$ are used to place the new poles according to

$$p_n^{\rm new} = (-\alpha \pm j)\,\omega_{\rm max}^n\,, \tag{13}$$

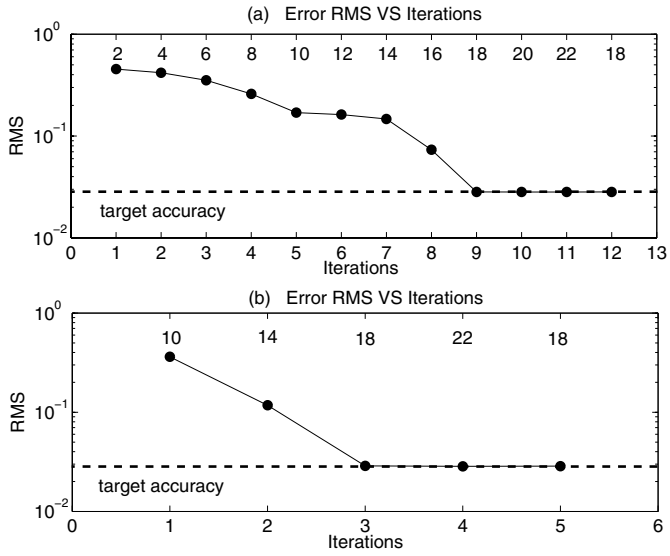

Fig. 4. Error $\widehat{\varepsilon}$ versus iterations for the example of Fig. 1a, for two different choices of controlling parameters. The top scale in each panel reports the number of macromodel poles ar each iteration.

with $\alpha \ll 1$. Only the frequencies corresponding to the largest peaks are considered. As shown in Fig. 3, the frequencies associated to the largest peaks (empty circles, bottom panel) have a one-to-one correspondence to the poles of the original function that have not yet been identified. This gives confidence for the automatization of this pole-placement scheme.

The new proposed algorithm is therefore very similar and has the same mathematical foundations of the standard VF scheme. However, at each iteration the approximation is first tested for spurious poles. Then, the number of poles is increased as described above, and the standard VF relocation (3) is applied. The iterations are stopped when the approximation error (8) stagnates. This condition is checked by comparing the achieved error to the error at previous iterations. Figure 4 reports the decay of the approximation error versus iterations, obtained by applying the algorithm to the test case of Fig. 1a, with two different parameter settings. Panel (a) uses the most conservative choice (small number of initial poles, small number of added poles per iteration). Panel (b) uses instead multiple pole addition at each iteration and a larger starting order. This choice results into a much smaller number of iterations to reach the noise floor. These plots should be compared with the corresponding error evolution for the standard VF reported in Fig. 2. The improvements are evident. A more precise description of the algorithm including all details can be found in [4].

V. Numerical results

A. A Monte Carlo robustness study

The robustness of the proposed macromodeling algorithm to noise is first investigated via a Monte Carlo analysis. Several noisy realizations resulting from addition of Gaussian noise to various cases of synthetic rational responses were generated.

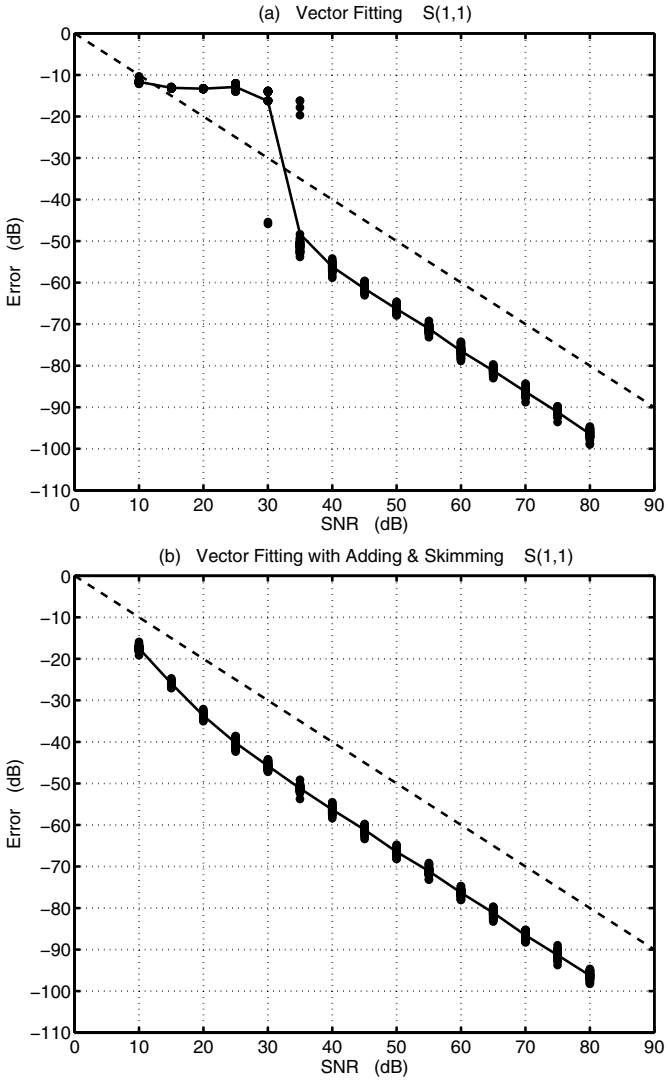

Fig. 5. Noise sensitivity of standard VF (a) and proposed algorithm (b) applied to a 30-pole two-port with normalized loss factor $\vartheta = 10^{-4}$. The identification error is plotted versus Signal to Noise Ratio. The cloud of dots represents the results obtained for each of 45 different realizations. The continuous lines are the average among all realizations. Dashed line is the $-\mathrm{SNR}_{\mathrm{dB}}$ threshold.

A very large number of numerical tests has been performed for many parameter combinations. We report here only the results for a representative case, corresponding to $N = 30$ poles, $P = 2$ ports, and loss factor $\vartheta = 10^{-4}$. Figure 5 reports the identification error obtained by standard VF and by the proposed algorithm for various noise levels. Note that the displayed error, defined as

$$\begin{aligned} \varepsilon_{ij} &= 10\log_{10}\frac{||S_{ij}^{\mathrm{fit}} - S_{ij}||^2}{||S_{ij}||^2} \\ &= -\mathrm{SNR}_{\mathrm{dB}} + 10\log_{10}\frac{||S_{ij}^{\mathrm{fit}} - S_{ij}||^2}{||N_{ij}||^2}, \end{aligned} \quad (14)$$

uses the "clean" and known rational function S_{ij} as the reference. This reference will obviously not be available in

practical applications. Panel (a) in the figure shows the results of standard VF. Only for SNR values more than 40 dB the standard VF has good performance. For higher noise levels, the convergence problems due to the spurious poles significantly affect the accuracy of the results, leading to very large identification errors. This is a clear indication of sensitivity to noise. Panel (b) shows the results of the proposed algorithm. The identification error is uniformly less than the $-\mathrm{SNR}_{\mathrm{dB}}$ threshold, for all tested noise levels. This indicates that the deviation between the model and the true rational function is much less than the noise itself, by as much as 10-15dB. This is a clear indication of robustness to noise. A complete report of the numerical tests will be found in [4].

B. Applications

Here we show practical applications of proposed algorithm. The first example is intended to illustrate the automatic order estimation capabilities. Fig. 6 illustrates a simplified geometry for the investigation of lumped and distributed coupling between power/ground conductors and signal conductors on typical PCB's. Ports 1 and 2 are located between the power and ground conductors, while ports 3–6 provide the termination to a coupled stripline structure. The structure was analyzed using a full-wave transient solver based on the Finite Integration technique [5]. In this simulation, the PCB was terminated on each side with perfect magnetic walls, and the reference impedance for each port was set to the standard value $R_0 = 50\ \Omega$. After application of Fast Fourier Transform to the transient data obtained by the field solver, the frequency-dependent 6×6 scattering matrix was obtained up to a maximum frequency of 3 GHz, with a total of $K = 1021$ samples per response.

Some of the scattering responses are depicted by continuous thin lines in Fig. 7. The resonances of the power/ground planes, clearly visible in $S_{1,1}$, are mainly determined by the board size and by the location of the power/ground ports. On the other hand, the responses of the coupled striplines are mainly determined by their cross-section and length (see $S_{3,3}$ and $S_{3,4}$). However, the power/ground resonances are also visible, to a lesser extent, in the stripline responses. These two sets of resonances are not directly related one to each other and may require different sets of poles in the macromodel. The correct order to employ in the rational approximation is far from evident using a priori considerations. The results of the proposed scheme are plotted in Fig. 7 with dashed lines. All the responses are fitted with excellent accuracy, since there is no visible difference between model and data. The maximum resulting deviation among all responses and all frequency samples is 5.2×10^{-3}, with a total number of 78 poles, which is automatically determined by the algorithm.

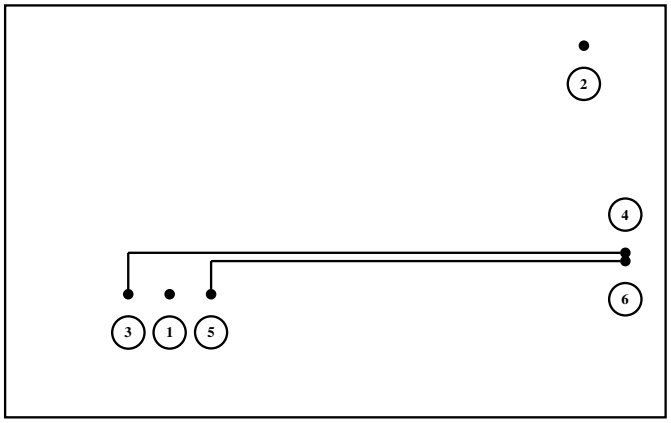

Fig. 6. PCB structure used as a benchmark for the new macromodeling scheme. The board size is 16×10 cm, with a power-signal-ground configuration ($\sigma = 5.8 \times 10^7$ S/m for all conductors). Each layer ($\varepsilon_r = 4.2$, $\tan\delta = 0.001$) is 0.7 mm high. The stripline conductors are 0.2 mm wide with a separation in the coupled segment of 0.5 mm. Port locations are, in mm units from the bottom-left corner, 1:(40,30), 2:(140,90), 3:(29,31), 4:(150,41.1), 5:(49,31), and 6:(150,40.6).

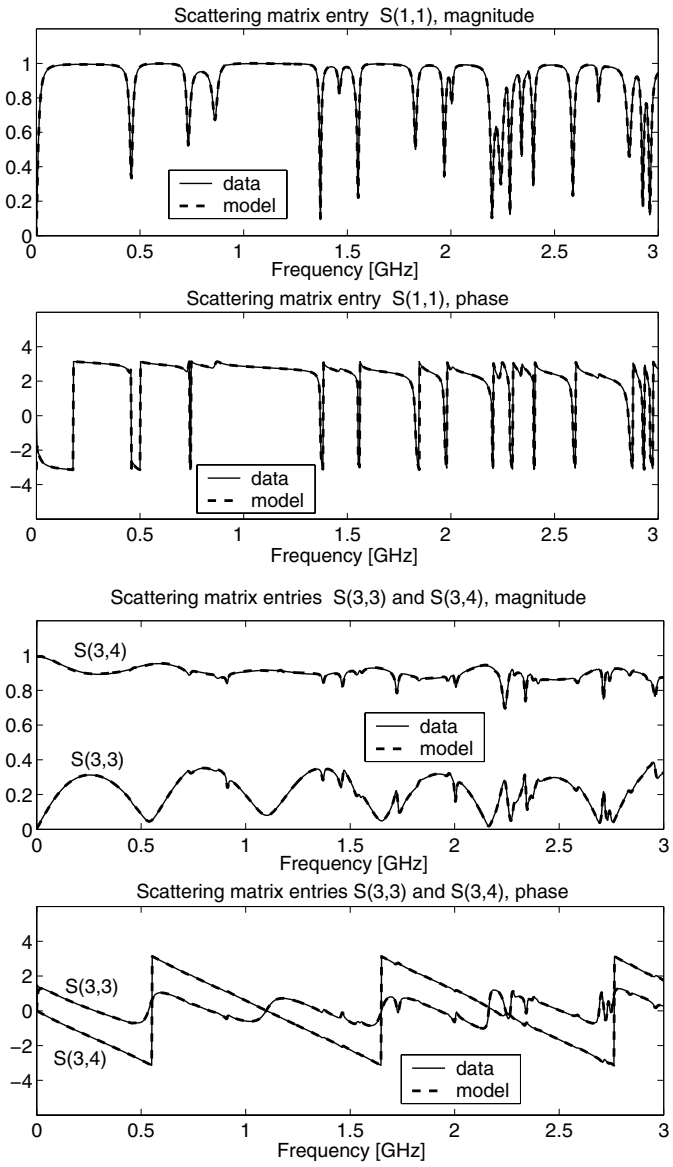

Fig. 7. Selected scattering responses for the structure depicted in Fig. 6.

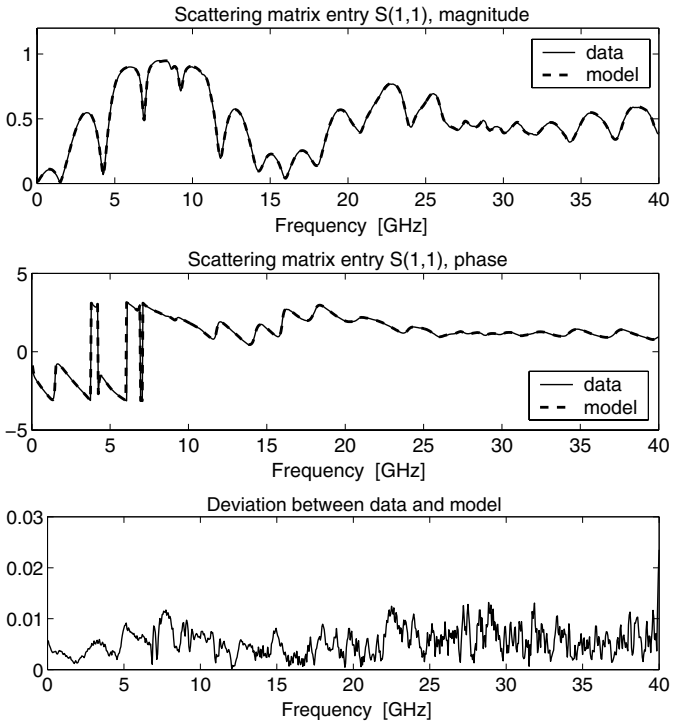

Fig. 8. Selected scattering responses of a 2 cm stripline including launches.

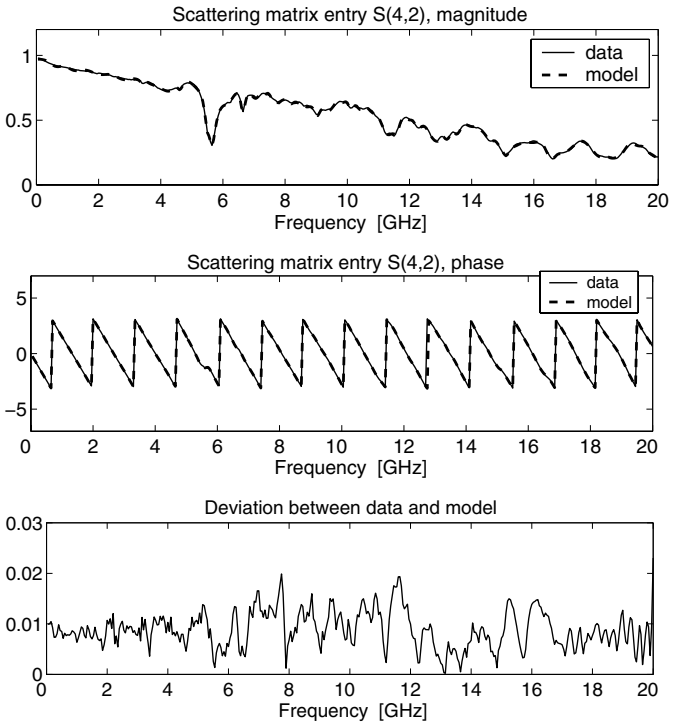

Fig. 9. Selected scattering responses of a connector.

We conclude the set of application examples by presenting two cases of macromodels generated from actual measurements. The first structure is a 2 cm stripline including the discontinuities caused by the signal launches. The second structure is a connector. We are unable to show the actual geometry due to a confidentiality agreement. The frequency-dependent scattering parameters for both structures were obtained via direct VNA measurements (courtesy of IBM) up to a maximum frequency of 40 GHz and 20 GHz, respectively. This extended frequency spectrum is required by an accurate Signal Integrity characterization for the the high-speed waveforms that are intended to propagate along these interconnects. Some selected responses of the two structures are depicted in Fig. 8 and Fig. 9, respectively. The top panels show a comparison between the generated model and the measured data. These plots show that the achieved accuracy is excellent. The deviation between model and data is hardly visible on the adopted scale. Therefore, we included also a plot of the frequency-dependent deviation $\Delta_{i,j}(\omega)$ in the bottom panels. These plots reveal also the presence of noise in the measurements, thus justifying the use of proposed fitting algorithm for the macromodel generation.

VI. Conclusion

We have presented an improved version of the standard Vector Fitting pole relocation algorithm for the generation of macromodels of linear interconnect structures. The new algorithm is based on the identification of spurious poles and on an incremental poles adding process. The combination of these features allows the automatic order estimation embedded into an iterative process that results quite robust to noise. The validations provided in this work show that, even with small signal to noise ratios, the new algorithm is highly efficient and reliable. Conversely, application of the standard VF iterations would result in poor or no convergence at all even in presence of small noise amounts. The application of the new algorithm to some interconnect structures and networks typically found in high-speed digital systems illustrates the excellent accuracy that can be achieved.

Acknowledgment

The Authors are grateful to C. Schuster of IBM for providing the measurements that were used for some of the test cases, and to CST GmbH for kindly providing a free academic license of Microwave Studio. This work is supported in part by the Italian Ministry of University (MIUR) under a Program for the Development of Research of National Interest (PRIN grant # 2004093025).

References

[1] B. Gustavsen, A. Semlyen, "Rational approximation of frequency responses by vector fitting", *IEEE Trans. Power Delivery*, Vol. 14, July 1999, pp. 1052–1061.

[2] B. Gustavsen (ed.), *The Vector Fitting WEB Site*, http://www.energy.sintef.no/Produkt/VECTFIT/index.asp

[3] B. Gustavsen, "Computer code for rational approximation of frequency dependent admittance matrices", *IEEE Trans. Power Delivery*, vol. 17, no. 4, pp. 1093-1098, Oct. 2002.

[4] S. Grivet-Talocia, M. Bandinu, "Improving the Convergence of Vector Fitting in Presence of Noise", submitted to *IEEE Transactions on Electromagnetic Compatibility*, Jan. 2005.

[5] *CST Microwave Studio Manual, version 4*, Computer Simulation Technology GmbH, Germany, 2003 (www.cst.de).